

## 1 Introduction

In the present paper, we consider an interface between two liquid layers subject to horizontal harmonic vibrations, of amplitude  $a$  and frequency  $\omega$ .

In experimental works by Bezdeneznykh *et al.* [1] and by Wolf [2] for a long horizontal reservoir filled with two immiscible viscous fluids, an interesting phenomenon was found at the interface: the horizontal vibrations lead to the formation of a steady relief. This formation mechanism has a threshold nature; it is noteworthy that such a wavy relief appears on the interface only if the densities of the two fluids are close enough, i.e. it does not appear for the liquid/gas interface (free surface). The interface is absolutely unstable if the heaviest fluid occupies the upper layer; i.e., the horizontal vibration does not prevent the evolution of Rayleigh-Taylor instability, in contrast to the vertical one which under certain conditions suppresses its evolution. A theoretical description of this phenomenon was provided by Lyubimov & Cherepanov [3] within the framework of a high frequency (of the vibration) approximation and an averaging procedure; they found that a horizontal vibration leads to a quasi-equilibrium state i.e., a state where the mean motion is absent but the interface oscillates with a small amplitude (of the order of magnitude of the cavity displacement) with respect to the steady relief. In particular, they found that the relief (in the case of a heavy fluid occupying the bottom layer) with finite wavelength is not possible for any thickness of fluid layers. In fact, the relief with finite wavelength arises only for considerably thick layers of height  $h > [3\alpha / (g(\rho_1 - \rho_2))]^{1/2}$ , where  $\alpha$  is the coefficient of surface tension,  $\rho_1$  and  $\rho_2$  are the densities of lower and upper layer, respectively;  $g$  is the gravity acceleration. In the approach [3], two parameters were assumed to be asymptotically small simultaneously: (i) the dimensionless thickness of the viscous skin-layers  $\delta = h^{-1}\sqrt{\nu/\omega}$ ,  $\nu$  being the kinematic viscosity and (ii) the dimensionless amplitude of the vibration  $\epsilon = a/h$ . But in the limiting case  $\epsilon \rightarrow 0$ , the possibility of description of parametric resonant effects is absent and only the basic instability mode (Kelvin–Helmholtz, of two counter flows) remains.

In this investigation, the condition  $\epsilon \rightarrow 0$  is dropped and the vibration frequency is considered as relatively low, thus the averaging method could no longer be applied.

## 2 Problem formulation

Let us consider the system of two immiscible, incompressible liquids filling rectangular cavity of length  $L$  and height  $h$ . In the state of rest the heavy liquid (of density  $\rho_1$ ) occupies

the bottom region of height  $h_1$ , and the light liquid (of density  $\rho_2$ ) – the upper region of height  $h_2$  ( $h = h_1 + h_2$ ). We choose Cartesian coordinate system in such a way that the  $x, y$ -axis lie in horizontal plane, the  $z$ -axis is directed vertically,  $z = 0$  corresponds to the unperturbed interface. Let the cavity perform harmonic oscillation along the  $x$ -axis, with the amplitude  $a$  and frequency  $\omega$ , and let  $\vec{\gamma}$  be the unit vector along the  $z$ -axis, while  $\vec{j}$  along the vibration axis (Fig. 1).

The waves are generated on the interface due to such oscillation, and propagate from the vertical endwalls to the central part of the cavity. But, if viscosities of the liquids are not too small, such a waves are damped on relatively short distances from the endwalls. For example, for transformer oil and glycerine in Earth gravity field and angular frequencies of the vibration of the order of magnitude  $10^2 Hz$ , the damping length  $l_d$  is of the order of magnitude of  $1\text{ mm}$ . In the following, we assume that the condition  $L \gg l_d$  is satisfied and we consider only the central part of the cavity, far away from the endwalls, which the interface waves generated near the endwalls do not reach. Therefore in the basic state the interface could be considered as plane and horizontal.

However, the liquid in the central part of the cavity can't stay at rest, and the velocities of the liquid motion in the bottom and upper layers must be different. Indeed, since the densities of liquids are different, then pressures gradients would be different if the velocities in the layers are equal. The latter is in contradiction with the normal stress balance condition at the interface. The only exception might be the case of liquids which stay in rest in laboratory reference frame, but such a situation is impossible because of the incompressibility conditions. To prove this, let us consider the cross-section of the cavity by the vertical plane  $S_{-+} = S_- + S_+$ , attached to the cavity (Fig. 1). Then liquid volume  $V = V_{r-} + V_{r+}$  to the right (for example) of the cross-section is constant. By virtue of the incompressibility the latter means that in the cavity frame the full liquid consumption through the  $S_{-+}$  must be zero:

$$\forall x : \int_{-h_1}^{\xi} v_{1x} dz + \int_{\xi}^{h_2} v_{2x} dz = 0 \quad (2.0)$$

where  $\xi$  is the vertical coordinate of the interface. We stress that the FULL consumption across any vertical cross-section is zero. At the same time the consumptions of individual liquids can be non-zero if the flow is unsteady because the interface is not at rest near the vertical endwalls, therefore the volume of each liquid to the right of the cross-section  $S_{-+}$  is

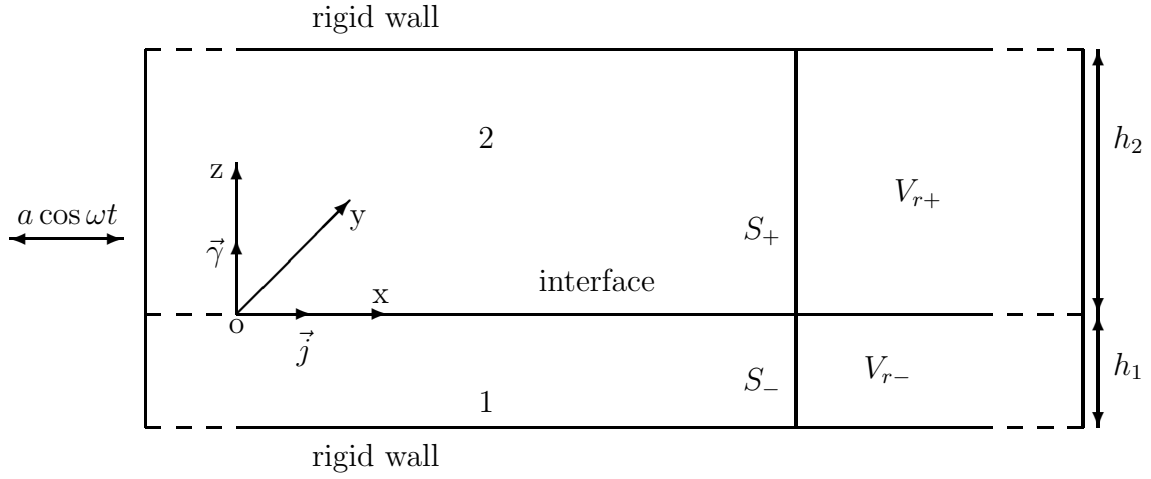


Fig. 1.

time-dependent. If the liquids stay in rest in the laboratory frame, then in (2.0) the velocities  $v_{1x}$  and  $v_{2x}$  are equal and (2.0) could not be satisfied. Thus, despite of the statement "in long cavity the interface waves generated near the endwalls do not penetrate into the central part of the cavity", the motion in the central part is always present and all of the above discussion gives the opportunity for the approximation of the infinite horizontal layer. Moreover, the condition (2.0) must be, of course, juncted.

The concrete flow in the inviscid case is obtained in Section 3, the flow in viscous case – in Section 4.2. We stress as early as in this Section that the basic flow, as is obvious from (2.0), is of counter-flow type, that makes us to expect the rise of Kelvin–Helmholtz instability, while the periodic character of the flow allows to expect the parametric resonance effects.

In the cavity frame, the Navier–Stokes equations for the motion could be obtained from the standard equations written in the laboratory frame by considering the total acceleration, i.e.

$$-g\vec{\gamma} \rightarrow -g\vec{\gamma} + a\omega^2\vec{j} \cos \omega t.$$

And so, the full Navier–Stokes equations read

$$\frac{\partial \vec{v}_\beta}{\partial t} + (\vec{v}_\beta \nabla) \vec{v}_\beta = -\frac{1}{\rho_\beta} \nabla p_\beta + \nu_\beta \Delta \vec{v}_\beta - g\vec{\gamma} + a\omega^2\vec{j} \cos \omega t \quad (2.1)$$

and the continuity equations for the two layers read

$$\text{div } \vec{v}_\beta = 0 \quad (2.2)$$

where the subscript  $\beta = 1, 2$  refers to the lower and upper layers, respectively; the other notation being conventional.

No-slip boundary conditions for the velocity are imposed on the rigid walls of the cavity

$$\text{at } z = -h_1 : \quad \vec{v}_1 = 0 \quad (2.3)$$

$$\text{at } z = h_2 : \quad \vec{v}_2 = 0 \quad (2.4)$$

and on the interface  $z = \xi(x, y, t)$ , the following conditions are satisfied:

- stress balance

$$(p_1 - p_2)n_i = (\sigma_{ik}^{(1)} - \sigma_{ik}^{(2)})n_k + \alpha n_i \operatorname{div} \vec{n} \quad (2.5)$$

- velocity continuity

$$\vec{v}_1 = \vec{v}_2 \quad (2.6)$$

- kinematic condition

$$\frac{\partial \xi}{\partial t} + (\vec{v}_1 \nabla) \xi = \vec{v}_1 \cdot \vec{\gamma} \quad (2.7)$$

In (2.5 - 2.7),  $\alpha$  is the coefficient of the surface tension,  $\sigma_{ik}^{(\beta)}$  are the viscous stress tensors:

$$\sigma_{ik}^{(\beta)} = \frac{\partial v_{\beta,i}}{\partial x_k} + \frac{\partial v_{\beta,k}}{\partial x_i}.$$

The integral condition of zero full consumption reads

$$\forall x : \quad \int_{-h_1}^{\xi} \vec{v}_1 \cdot \vec{j} \, dz + \int_{\xi}^{h_2} \vec{v}_2 \cdot \vec{j} \, dz = 0 \quad (2.8)$$

### 3 Inviscid approximation

After omitting the viscous term the Navier–Stokes equations (2.1) read:

$$\frac{\partial \vec{v}_\beta}{\partial t} + (\vec{v}_\beta \nabla) \vec{v}_\beta = -\frac{1}{\rho_\beta} \nabla p_\beta - g \vec{\gamma} + a \omega^2 \vec{j} \cos \omega t \quad (3.1)$$

The continuity equations remain unaltered:

$$\operatorname{div} \vec{v}_\beta = 0 \quad (3.2)$$

The impermeability boundary conditions are imposed on the rigid walls instead of the no-slip conditions:

$$\text{at } z = -h_1 : \quad \vec{v}_1 \cdot \vec{\gamma} = 0 \quad (3.3)$$

$$\text{at } z = h_2 : \quad \vec{v}_2 \cdot \vec{\gamma} = 0 \quad (3.4)$$

On the interface  $z = \xi(x, y, t)$  the following conditions are imposed:

- normal stress balance

$$p_1 - p_2 = \alpha \operatorname{div} \vec{n} \quad (3.5)$$

- continuity of normal components of velocity

$$\vec{v}_1 \cdot \vec{n} = \vec{v}_2 \cdot \vec{n} \quad (3.6)$$

- kinematic condition

$$\frac{\partial \xi}{\partial t} + (\vec{v}_1 \nabla) \xi = \vec{v}_1 \cdot \vec{\gamma} \quad (3.7)$$

The zero full consumption condition (2.8) remains unaltered.

The problem (3.1) - (3.7), (2.8) admits a solution of the form:

$$\vec{V}_\beta = U_\beta \vec{j} \sin \omega t \quad (3.8)$$

where

$$U_1 = a\omega \frac{h_2(\rho_1 - \rho_2)}{h_1\rho_2 + h_2\rho_1} = a\tilde{U}_1 \quad \text{and} \quad U_2 = -a\omega \frac{h_1(\rho_1 - \rho_2)}{h_1\rho_2 + h_2\rho_1} = a\tilde{U}_2 \quad (3.9)$$

The corresponding pressure field is given by the expression

$$p_\beta = -\rho_\beta g z + a\omega^2 \rho_1 \rho_2 \frac{h_1 + h_2}{h_1\rho_2 + h_2\rho_1} x \cos \omega t \quad (3.10)$$

The above solution corresponds to a plane-parallel, unsteady, counter flow which keeps the interface flat ( $\xi = 0$ ). Note that in the case of equal densities,  $\vec{V}_1$  and  $\vec{V}_2$  tend to zero, i.e. fluids stay at rest in the cavity frame. In the case  $\rho_2 \ll \rho_1$ , the lower fluid stays at rest in the laboratory frame ( $U_1 = a\omega$ ).

Thus, in the inviscid case we deal with the stability problem for the interface between two counter flows, and the difference in the flows velocities is a periodic function of time. Linear

stability problem could be reduced to the ordinary differential equation for the amplitude  $\xi(t)$  of the interface displacement from quasi-equilibrium horizontal position:

$$(F_1 + F_2) \frac{d^2 \xi}{dt^2} + 2ik \frac{d\xi}{dt} (F_1 U_1 + F_2 U_2) \sin \omega t + \xi (\alpha k^3 + (\rho_1 - \rho_2) g k + i(F_1 U_1 + F_2 U_2) k \omega \cos \omega t - k^2 (F_1 U_1^2 + F_2 U_2^2) \sin^2 \omega t) = 0, \quad (3.11)$$

$$\text{with} \quad F_1 = \rho_1 \coth(kh_1) \quad \text{and} \quad F_2 = \rho_2 \coth(kh_2)$$

In (3.11),  $k$  is the wavenumber of the disturbances, which determines the periodicity of the solution along vibration axis. It is straightforward to show that stability problem admits the analogue of Squire's theorem [4]. The latter gives the possibility of considering only plane (2D) disturbances.

It is convenient to eliminate from (3.11) the term which contains the first order derivative in  $\xi$ . To do so, we make the change of variable [5]

$$\xi(t) = Y(t) e^{i\Phi(t)} \quad (3.12)$$

where

$$\Phi = \frac{k}{\omega} \frac{F_1 U_1 + F_2 U_2}{F_1 + F_2} \cos \omega t \quad (3.13)$$

(since  $\Phi$  is real, then  $\xi$  and  $Y$  are equal via a modulus, i.e.  $\xi$  and  $Y$  are equivalent from the point of view of stability). This results in the standard Mathieu equation for  $Y$ :

$$\frac{d^2 Y}{dt^2} + (A - Q \cos^2 t) Y = 0 \quad (3.14)$$

The equation (3.14) is in dimensionless form, with the following reference quantities for time and length:

$$t^* = 1/\omega \quad \text{and} \quad l^* = l_c = [\alpha / (g(\rho_1 - \rho_2))]^{1/2}$$

where  $l_c$  is the capillary length, and with the following notation:

$$Q = \frac{4B_v k^2}{We_1} \frac{\rho \coth(kH_1) \coth(kH_2)}{(\rho \coth(kH_1) + \coth(kH_2))^2} \frac{(H_1 + H_2)^2 (\rho - 1)^2}{(H_1 + H_2 \rho)^2} \quad (3.15)$$

$$A = \frac{k(1 + k^2)}{We_1} \frac{\rho - 1}{\rho \coth(kH_1) + \coth(kH_2)} \quad (3.16)$$

In formulas (3.15) and (3.16),  $We_1 = \omega^2 l_c / g$  is Weber number based on the capillary length,  $\rho = \rho_1 / \rho_2$  is densities ratio,  $H_1 = h_1 / l_c$  and  $H_2 = h_2 / l_c$  are dimensionless layer thicknesses. We also introduced the dimensionless parameter  $B_v$ , characterizing the vibrations intensity:

$$B_v = \frac{a^2 \omega^2}{4} \left( \frac{\rho_1 - \rho_2}{g \alpha} \right)^{1/2}.$$

The solutions of the equation (3.14), which correspond to the neutral boundary, form two classes:  $Y_+$ , having period  $2\pi$  (harmonic disturbances) and  $Y_-$ , having period  $\pi$  (subharmonic disturbances). The solutions of subharmonic type are antiperiodic, that means that they change the sign for a shift of  $\pi$ .

We plot the boundaries of the instability regions (obtained by numerical integration of the Mathieu equation (3.14)) in terms of the two parameters,  $B_v$  and  $k$ . The neutral curves shown in Fig. 2, 3 correspond to Weber numbers equal respectively to  $We_1 = 10$  and  $We_1 = 100$  ( $H_1 = H_2 = 1, \rho = 2$ ).

The left curve in this Figures bounds Kelvin–Helmholtz instability region. In the referred case  $H_1 = H_2 = 1$  the most dangerous are longwave disturbances with  $k = 0$ . In [3] was investigated the case  $We_1 \rightarrow \infty$  with finite heights of the layers. It was found that if  $H_1 = H_2 = H$  then the transition from the longwave instability to the finite wavelength instability occurs at  $H = H_* = \sqrt{3}$ . It is straightforward to analyse the case of finite  $We_1$ . Note, that if  $k$  is small, then  $Q$  and  $A$  are small also, and could be expanded into power series in  $k$ . The result is that at  $H < H_*$  the longwave instability takes place at any values of  $We_1$ , but at  $H > H_*$  only for

$$We_1 < \frac{3}{8} \frac{H}{H^2 - 3} \frac{\rho - 1}{\rho + 1} \quad (3.17)$$

In the instability region discussed, the instability mechanism is, in fact, the same as in the standard case of Kelvin–Helmholtz instability: the velocity grows up and the pressure falls down over the elevations of the interface. The consequence of this is the reducing of the effective stiffness of the system and, starting from some threshold, the rise of the instability. As shown in [3], in the case of high frequencies of the vibration the nonlinear development of such instability results in the formation of a quasi-stationary wave relief on the interface.

However, periodic changes of the velocity can result not only in the average effect, but in the resonance amplification of eigenoscillations. Inasmuch as in the absence of the dissipation

the eigenoscillations are not damped, then the instability will take place at infinitely small amplitude of the vibration (if the synchronism condition is satisfied). On Fig. 2, 3 the regions of parametric instability approach the abscissa as narrow ends ("tongues"); the points  $k_n$  at which the  $n$ -th region of instability is in contact with the  $k$ -axis can be evaluated from the equation  $A = n^2, n = 1, 2, \dots$ . As the vibration frequency grows, i.e. as Weber number increases, the points  $k_n$  shift to the shortwave region (as seen from Fig. 2,3) and in the limit  $We_1 \rightarrow \infty$  they are displaced into infinity. Thus, at high frequencies of the vibration the parametric instability can take place only for shortwave disturbances but, for such disturbances, the viscosity could not be ignored. It has to be expected that for big values of Weber number only the quasi-static instability must be observed, with mechanism of excitation which is weakly sensitive to the viscosity.

## 4 2D linear stability problem for viscous fluids

To simplify the following presentation, we assume in this Section that the two layers are of equal height  $h_1 = h_2 = h$ . In addition, we non-dimensionalize the problem using the scales

$$t^* = 1/\omega; \quad l^* = h; \quad u^* = a\omega; \quad p^* = \rho_2 h a \omega^2$$

### 4.1 Problem formulation

The following dimensionless equations replace the equations (2.1) - (2.8):

$$\frac{\partial \vec{v}_\beta}{\partial t} + A(\vec{v}_\beta \nabla) \vec{v}_\beta = -R_\beta \nabla p_\beta + \Omega_\beta^{-1} \Delta \vec{v}_\beta - G_o A^{-1} \vec{\gamma} + \vec{k} \cos t \quad (4.1)$$

$$\operatorname{div} \vec{v}_\beta = 0 \quad (4.2)$$

$$\text{at } z = -1 : \quad \vec{v}_1 = 0 \quad (4.3)$$

$$\text{at } z = 1 : \quad \vec{v}_2 = 0 \quad (4.4)$$

$$\text{at } z = \xi(x, y, t) : \quad [p]n_i = (\Omega_1^{-1} \rho \sigma_{ik}^{(1)} - \Omega_2^{-1} \sigma_{ik}^{(2)})n_k + A^{-1} We_2^{-1} n_i \operatorname{div} \vec{n} \quad (4.5)$$



$$[\vec{v}] = 0 \quad (4.6)$$

$$\frac{1}{A} \frac{\partial \xi}{\partial t} + (\vec{v}_1 \nabla) \xi = \vec{v}_1 \cdot \vec{\gamma} \quad (4.7)$$

$$\forall x : \quad \int_{-1}^{\xi} \vec{v}_1 \cdot \vec{j} \, dz + \int_{\xi}^1 \vec{v}_2 \cdot \vec{j} \, dz = 0 \quad (4.8)$$

Here and below, the quantity jump across the interface is denoted by square brackets, for example  $[p] = p_1 - p_2$ , and the following parameters are introduced:

$$A = ah^{-1}; \Omega_\beta = h^2 \omega \nu_\beta^{-1}; G_o = g/(h\omega^2); We_2 = \rho_2 h^3 \omega^2 / \alpha; \rho = \rho_1 / \rho_2; R_1 = 1/\rho \text{ and } R_2 = 1.$$

So, the system of equations governing the fluid motion contains 7 dimensionless parameters:  $A$  is dimensionless amplitude,  $\Omega_\beta$  are dimensionless frequencies, the parameter  $G_o$ ,  $We_2$  is a new Weber number,  $k$  is the wave number and  $\rho$  is the densities ratio.

## 4.2 Solution method

The system of equations (4.1) - (4.8) admits a solution of the form

$$\vec{V}_\beta = U_\beta(z) \vec{j} \exp(it) + C.C. \quad (4.9)$$

$$P_\beta = -G_o A^{-1} R_\beta^{-1} z + x(S \exp(it) + C.C.), \quad S = const. \quad (4.10)$$

The above solution corresponds to the plane-parallel unsteady counter flow which keeps the interface flat ( $\xi = 0$ ) (to be compared with (3.8)-(3.10) in the inviscid case). The function  $U_\beta(z)$  could be found analytically, but its expression is too complicated, so it was determined numerically. Figure 4 represents the velocity profiles at four time instants: (a)  $t = 0$ , (b)  $t = \pi/2$ , (c)  $t = \pi$ , (d)  $t = 3\pi/2$ . The direction of the flow changes every half period of the external forcing. Note the thin boundary layers at both sides of the interface and near the walls ( Figs. 4a, 4c).

For the reasons discussed in Section 3, we investigate the stability of the basic state (4.9), (4.10) with respect to periodic (in time and space) 2D disturbances. If the vibration

frequency is high enough, then thin boundary layers occur at the interface (on both sides) and near the two horizontal walls, making the task of numerical solution particularly complicated.

After linearizing near the solution (4.9) and (4.10), the Navier–Stokes equations for small disturbances  $\vec{u}_\beta$  and  $p_\beta$  are:

$$\frac{\partial \vec{u}_\beta}{\partial t} + A(\vec{V}_\beta \nabla) \vec{u}_\beta + A(\vec{u}_\beta \nabla) \vec{V}_\beta = -R_\beta \nabla p_\beta + \Omega_\beta^{-1} \Delta \vec{u}_\beta \quad (4.11)$$

$$\text{div } \vec{u}_\beta = 0 \quad (4.12)$$

Boundary conditions for the system (4.11) - (4.12) read:

$$\text{at } z = -1 : \quad \vec{u}_1 = 0 \quad (4.13)$$

$$\text{at } z = 1 : \quad \vec{u}_2 = 0 \quad (4.14)$$

$$\text{at } z = 0 : \quad A^{-1} \left( (1 - \rho) G_o \xi + W e_2^{-1} \Delta \xi \right) n_i + [p] n_i = (\Omega_1^{-1} \rho \sigma_{ik}^{(1)} - \Omega_2^{-1} \sigma_{ik}^{(2)}) n_k \quad (4.15)$$

$$[\vec{u}] = - \left[ \frac{\partial \vec{V}}{\partial z} \right] \xi \quad (4.16)$$

$$\frac{1}{A} \frac{\partial \xi}{\partial t} + (\vec{V}_1 \nabla) \xi = u_{1z} \quad (4.17)$$

This is valid as long as the deformation  $\xi$  is small compared to the wavelength of the instability.

It is easy to see that the problem is uniform in  $x$ -direction. This allows us to consider only normal disturbances. The linear stability problem is now summarized as:

$$\frac{\partial u_\beta}{\partial t} + ik A V_\beta u_\beta + w_\beta A \frac{\partial V_\beta}{\partial z} = -ik R_\beta p_\beta + \Omega_\beta^{-1} \left( \frac{\partial^2}{\partial z^2} - k^2 \right) u_\beta \quad (4.18)$$

$$\frac{\partial w_\beta}{\partial t} + ik A V_\beta w_\beta = -R_\beta \frac{\partial p_\beta}{\partial z} + \Omega_\beta^{-1} \left( \frac{\partial^2}{\partial z^2} - k^2 \right) w_\beta \quad (4.19)$$

$$iku_\beta + \frac{\partial w_\beta}{\partial z} = 0 \quad (4.20)$$

$$\text{at } z = -1 : \quad u_1 = w_1 = 0 \quad (4.21)$$

$$\text{at } z = 1 : \quad u_2 = w_2 = 0 \quad (4.22)$$

$$\text{at } z = 0 : \quad A^{-1}\xi \left( (1 - \rho)G_o - W e_2^{-1}k^2 \right) + [p] + 2 \left( \Omega_2^{-1} \frac{\partial w_2}{\partial z} - \Omega_1^{-1} \rho \frac{\partial w_1}{\partial z} \right) = 0 \quad (4.23)$$

$$-\frac{\Omega_2}{\Omega_1} \rho \left( ikw_1 + \frac{\partial u_1}{\partial z} + \xi \frac{\partial^2 V_1}{\partial z^2} \right) + ikw_2 + \frac{\partial u_2}{\partial z} + \xi \frac{\partial^2 V_2}{\partial z^2} = 0 \quad (4.24)$$

$$[u] = - \left[ \frac{\partial V}{\partial z} \right] \xi \quad (4.25)$$

$$[w] = 0 \quad (4.26)$$

$$\frac{1}{A} \frac{\partial \xi}{\partial t} + ikV_1 \xi = w_1 \quad (4.27)$$

All fields could be expanded in time in Fourier series of the form

$$f_\beta(z, t) = \sum_{n=-\infty}^{\infty} f_{n\beta}(z) \exp(int) + C.C.,$$

where  $n$  might be taken integer, as well as half-integer. By keeping only a finite number of terms of the expansion in both fluids we get 2-point boundary value problems (BVP's, coupled through the conditions (4.23) - (4.27)), for the system of ordinary differential equations for the complex amplitudes  $p_{n\beta}(z)$ ,  $u_{n\beta}(z)$ ,  $w_{n\beta}(z)$  (note that  $\xi_n(z)$  may be eliminated from (4.23)-(4.27)). The coefficients in the equations depend on  $z$ , therefore the system could be resolved only numerically.

One important feature of the resulting ODE's systems is that integer and half-integer harmonics are not coupled (since the basic flow (4.9) introduce only a shift of  $\pm 1$  for  $n$  in (4.18)-(4.27)). So, finally, the corresponding BVP's can be solved independently. The

solutions of the BVP's involving integer harmonics have the same period as that of the forcing vibration (harmonic, or synchronous case) and the solutions of the BVP's involving half-integer harmonics have a period twice as that of the forcing vibration (subharmonic, or asynchronous case).

BVP's, in turn, allow the reduction to initial values problems (IVP's). We focus our attention on the synchronous case, since asynchronous solutions were not detected in the numerical investigation. The numerical procedure is described in [6].

## 5 Numerical results

The linear stability of the flat interface has been calculated using 21 basis functions  $f_n(z)$  in both cases (synchronous and asynchronous). Ten to twelve basis functions are enough to get sufficiently accurate numerical results if the dimensionless frequency is not high ( $\Omega < \approx 250$ ). The number of basis functions has to be increased if  $\Omega > 250$ .

In Figure 5, we show the neutral stability curves which divide the  $(k, A)$ -plane into regions of stable solutions, and regions (tongues) of unstable (exponentially growing in time) solutions. The values of the nondimensional parameters are  $\rho=2$ ,  $G_o=0.16$  and  $W e_2=6.25$ . Only synchronous solutions were detected. This situation is not unique (for the review and discussion see [7]). Asymptotic "inviscid" curves are plotted with solid lines, while the curves obtained numerically for viscous fluids at different values of the dimensionless frequency  $\Omega_1 = \Omega_2 = \Omega$ , are plotted with dashed lines (note that  $\Omega_1 = \Omega_2$  correspond to  $\nu_1 = \nu_2$ ).

For the high values of  $\Omega$  (corresponding to small viscosities) the numerical curves approach the bottom of the asymptotic tongues, which correspond to an instability threshold, but lower and lower (Fig. 5). As  $\Omega$  decreases (or the viscosities increase), the instability threshold grows (Fig. 6). We state that viscosity has a weak influence on the Kelvin–Helmholtz instability, but strongly damps the parametric instability associated with the excitation of capillary-gravity waves. In addition, as seen in Figures 5,6, at some critical frequency  $100 < \Omega_* < 250$ , the boundary of Kelvin–Helmholtz instability region unites with the boundary of the resonant zone, so that at smaller frequencies there exists a single neutral curve corresponding to each frequency value. This means that in the case of rather viscous fluids the difference between the parametric and non-parametric instabilities vanishes.

## FIGURES CAPTIONS

Fig. 1. Problem configuration.

Fig. 2. Neutral stability diagram (inviscid case), for  $We_1 = 10$ .

Unstable tongues touch the  $k$ -axis at points  $k_n$ , defined by the equation (3.28). The bigger is the tongue's number, the narrower it is.

The tongues shift towards shortwave region as the vibration frequency increases (next figure).

Fig. 3. Neutral stability diagram (inviscid case), for  $We_1 = 100$ .

The comparison of this Figure and Figure 2 reveals that the influence of changes in the vibration frequency on Kelvin-Helmholtz instability is very small.

Fig. 4. Velocity profile at four time instants (viscous case):

(a)  $t = 0$ , (b)  $t = \pi/2$ , (c)  $t = \pi$ , (d)  $t = 3\pi/2$ .

Flow direction changes every half period of the forcing vibration.

Fig. 5. Neutral stability  $k - A$  diagram (viscous case).

Parameters are:  $\rho=2$ ,  $G_o=0.16$  and  $We_2=6.25$ ;

$\Omega$  is large (250, 360), i.e., viscosity is small .

Fig. 6. Neutral stability  $k - A$  diagram (viscous case). Parameters are

the same as in Fig. 5;  $\Omega$  is small (25, 50, 100), i.e.,

viscosity is large. Viscosity makes weak influence on Kelvin-Helmholtz type instability but strongly damps the parametric instability.

In the case of rather viscous fluids, the difference between the parametric and non-parametric instabilities vanishes.

## References

- [1] *N.A.Bezdenezhnykh et al.*, 1984. Control of the fluid interface stability by vibration, electric and magnetic fields. III All-Union Seminar on hydromechanics and heat/mass transfer in microgravity. Chernogolovka, pp.18-20 (in Russian).
- [2] *G.H.Wolf*, 1969. The dynamic stabilization of the Rayleigh -Taylor instability and the corresponding dynamic equilibrium. *Z. Physik*, B. 227, N 3, S. 291-300.
- [3] *D.V.Lyubimov, A.A.Cherepanov*, 1987. Development of a steady relief at the interface of fluids in a vibrational field. *Fluid Dynamics*, vol. 22, pp. 849-854.
- [4] *H.B.Squire*, 1933. On the stability for three-dimensional disturbances of viscous fluid flow between parallel walls. *Proc. Roy. Soc.*, A142, 947, p. 621.
- [5] *D.V.Lyubimov, M.V.Khenner, M.M.Shotz*, 1998. Stability of a fluid interface under tangential vibrations. *Fluid Dynamics*, vol.33, N.3, pp.318-323.
- [6] *G.Z.Gershuni, E.M.Zhukhovitsky*, 1972. Convective stability of incompressible fluid. M.: Nauka, 392 p. (in Russian).
- [7] *A.C.Or*, 1997. Finite-wavelength instability in a horizontal liquid layer on an oscillating plane. *J. Fluid Mech.*, vol. 335, pp. 213-232.

This figure "figure2.gif" is available in "gif" format from:

<http://arxiv.org/ps/physics/9908007v1>

This figure "figure3.gif" is available in "gif" format from:

<http://arxiv.org/ps/physics/9908007v1>



This figure "figure4.gif" is available in "gif" format from:

<http://arxiv.org/ps/physics/9908007v1>

This figure "figure5.gif" is available in "gif" format from:

<http://arxiv.org/ps/physics/9908007v1>

This figure "figure6.gif" is available in "gif" format from:

<http://arxiv.org/ps/physics/9908007v1>